

# The contact value approximation for the pair distribution function of the inhomogeneous hard-sphere fluid

Paho Lurie-Gregg, Jeff B. Schulte, and David Roundy  
*Department of Physics, Oregon State University, Corvallis, OR 97331*

We introduce an approximation for the pair distribution function of the inhomogeneous hard sphere fluid. Our approximation makes use of our recently published averaged pair distribution function at contact which has been shown to accurately reproduce the averaged pair distribution function at contact for inhomogeneous density distributions. We further develop a separable form of this approximation that achieves greater computational efficiency by using exclusively fixed-kernel convolutions and thus allowing an implementation using fast Fourier transforms. We compare results for both versions of our pair distribution approximation with two previously published works and Monte-Carlo simulation, showing favorable results.

## I. INTRODUCTION

The standard approach in liquid state theory is to model a liquid as a hard-sphere reference fluid with attractive interactions that are treated perturbatively [1]. Recent advances have extended these perturbative approaches to inhomogeneous density distributions—that is, liquid interfaces—through the use of classical density functional theory (DFT), in which the grand free energy is found by minimizing a free energy functional of the density [2–10]. The perturbation theory treatment of intermolecular interactions relies on the pair distribution function of the reference fluid:  $g_{HS}^{(2)}(\mathbf{r}_1, \mathbf{r}_2)$ . Unlike the radial distribution function of a homogeneous fluid, there does not currently exist a tractable form for the pair distribution function of an inhomogeneous hard-sphere fluid, suitable for use in constructing a density functional [2, 3].

At its core, thermodynamic perturbation theory—sometimes referred to as the cluster, or high-temperature expansion—is an expansion of the free energy in powers of a small parameter, which is typically a pairwise attractive interaction:

$$F = F_0 + F_1 + \beta F_2 + \mathcal{O}(\beta^2) \quad (1)$$

where the terms  $F_n$  are corrections to the free energy of order  $n$  in the small interaction. The first and largest term in this expansion is

$$F_1 = \frac{1}{2} \iint g_{HS}^{(2)}(\mathbf{r}_1, \mathbf{r}_2) n(\mathbf{r}_1) n(\mathbf{r}_2) \Phi(|\mathbf{r}_1 - \mathbf{r}_2|) d\mathbf{r}_1 d\mathbf{r}_2 \quad (2)$$

where  $g_{HS}^{(2)}(\mathbf{r}_1, \mathbf{r}_2)$  is the pair distribution function of the hard-sphere reference fluid, and  $\Phi(r)$  is the pair potential. In this paper, we introduce a contact value approximation (CVA) for the hard-sphere pair distribution function which is suitable for use in the creation of classical density functionals based on thermodynamic perturbation theory. We then demonstrate a more computationally efficient separable version of the contact value approximation (CVA-S), which is based on a fit to the radial distribution function that is separable in a way that will enable efficient evaluation of the integral in Eq. 2.

## II. PREVIOUS THEORETICAL APPROACHES

The classic (and earliest) approach for computing the pair distribution function is to use Percus’ trick of treating one sphere as an external field, and to use the resultant equilibrium density to find the pair distribution function [1]. This elegant approach lends itself to DFT, and can be used to compute and plot the pair distribution function, but requires a full free-energy minimization *for each position*  $\mathbf{r}_1$  in  $g^{(2)}(\mathbf{r}_1, \mathbf{r}_2)$ , and hence would be prohibitively expensive as a tool in constructing a free energy functional.

The canonical inhomogeneous configuration for the hard-sphere fluid is the system consisting of a hard sphere at a hard wall. In 1986, Plischke and Henderson solved the pair distribution function of this system using integral equation theory under the Percus-Yevick approximation [11]. Ten years later, Götzelmann *et al.* found the pair distribution function near a hard wall by solving the Ornstein-Zernike equation using the direct correlation function found from a functional derivative of a classical DFT free energy functional [12]. Unfortunately, solving the inhomogeneous Ornstein-Zernike equation is computationally challenging, although more efficient approximate algorithms have been developed [13].

Another inhomogeneous configuration that is of interest is the test-particle configuration, in which one hard sphere is fixed. Where the hard-wall is a surface with no curvature, the test-particle configuration has a surface with curvature at the molecular length scale. In this case, the density gives the pair distribution function—this is just Percus’ trick—and the pair distribution function of this inhomogeneous test-particle system gives the triplet distribution function of the homogeneous fluid. The triplet distribution function of the homogeneous fluid has been computed by González *et al.* using the test-particle approach with *two* spheres fixed [14].

Lado recently introduced a new and improved efficient algorithm for implementing integral equation theory for inhomogeneous fluids, which computes  $g^{(2)}(\mathbf{r}_1, \mathbf{r}_2)$  [15]. While this approach is two orders of magnitude more efficient than previous implementations, it remains a computationally expensive approach, and unsuitable for re-

peated evaluation within a free-energy minimization.

### III. PREVIOUS APPROXIMATIONS TO THE PAIR DISTRIBUTION FUNCTION

There are several analytic approximations for the inhomogeneous pair distribution function, which extend the radial distribution function to inhomogeneous scenarios. These works differ in what density is used when evaluating the radial distribution function  $g(r, \eta)$ .

Several recent works [3, 4] have assumed a mean-density approximation for the pair distribution function:

$$g^{(2)}(\mathbf{r}_1, \mathbf{r}_2) \approx g\left(r_{12}, \frac{\pi\sigma^3}{6} \frac{1}{2}(n(\mathbf{r}_1) + n(\mathbf{r}_2))\right) \quad (3)$$

where  $g(r, \eta)$  is the radial distribution function as a function of radius and packing fraction  $\eta$ , and  $\sigma$  is the hard-sphere diameter. This approach, however, cannot be applied to highly inhomogeneous systems such as a dense fluid at a solid surface. These systems exhibit large density oscillations that lead to mean packing fractions greater than unity, which cannot occur in the bulk reference system that defines  $g(r, \eta)$ . The above papers restricted themselves to the liquid-vapor interface, which does not exhibit this pathology.

Non-pathological approaches use an average of the density over some volume. Fischer and Methfessel [16] introduce the approximation:

$$g^{(2)}(\mathbf{r}_1, \mathbf{r}_2) \approx g\left(r_{12}, n_3\left(\frac{1}{2}(\mathbf{r}_1 + \mathbf{r}_2)\right)\right) \quad (4)$$

where  $n_3$  is one of the fundamental measures defined in Fundamental Measure Theory [17], which is an integral of the density over a spherical volume:

$$n_3(\mathbf{r}) = \int n(\mathbf{r}') \Theta\left(\frac{1}{2}\sigma - |\mathbf{r} - \mathbf{r}'|\right) d\mathbf{r}' \quad (5)$$

Equation 4 is computationally awkward, because it treats as special the midpoint  $\frac{1}{2}(\mathbf{r}_1 + \mathbf{r}_2)$ . Moreover, the approach of Fischer and Methfessel is intended to approximate the pair distribution function only at contact, when the distance between  $\mathbf{r}_1$  and  $\mathbf{r}_2$  is the hard-sphere diameter.

Sokolowski and Fischer addressed the shortcomings of the theory of Fischer and Methfessel by modifying this approach to use averages, centered on the two points  $\mathbf{r}_1$  and  $\mathbf{r}_2$ :

$$g^{(2)}(\mathbf{r}_1, \mathbf{r}_2) \approx g\left(r_{12}, \frac{1}{2}(\bar{n}(\mathbf{r}_1) + \bar{n}(\mathbf{r}_2))\right) \quad (6)$$

where their averaged density  $\bar{n}(\mathbf{r})$  is given by:

$$\bar{n}(\mathbf{r}) \equiv \frac{3}{4\pi(0.8\sigma)^3} \int n(\mathbf{r}') \Theta(0.8\sigma - |\mathbf{r} - \mathbf{r}'|) d\mathbf{r}' \quad (7)$$

is the density averaged over a sphere with diameter  $0.8\sigma$  [18]. The value 0.8 in this formula was arrived at by fitting to Monte Carlo simulation. Although Eq. 6 has

the advantages of only involving density averages at the points at which the pair distribution function is desired, it cannot be written as a single-site convolution, since the convolution kernel depends on both points.

In a previous paper [19], we introduced a functional that gives a good approximation for the pair distribution function averaged over positions  $\mathbf{r}_2$  that are in contact with  $\mathbf{r}_1$ , defined as:

$$g_\sigma(\mathbf{r}_1) \equiv \frac{\int g^{(2)}(\mathbf{r}_1, \mathbf{r}_2) \delta(\sigma - |\mathbf{r}_1 - \mathbf{r}_2|) n(\mathbf{r}_2) d\mathbf{r}_2}{\tilde{n}(\mathbf{r}_1)} \quad (8)$$

where the weighted density  $\tilde{n}(\mathbf{r}_1)$  is defined by:

$$\tilde{n}(\mathbf{r}) \equiv \int n(\mathbf{r}') \delta(\sigma - |\mathbf{r} - \mathbf{r}'|) d\mathbf{r}'. \quad (9)$$

We use the contact-value theorem to derive the exact formula:

$$g_\sigma(\mathbf{r}) = \frac{1}{2} \frac{1}{k_B T n(\mathbf{r}) \tilde{n}(\mathbf{r})} \frac{\delta F_{HS}}{\delta \sigma(\mathbf{r})} \quad (10)$$

where  $\sigma(\mathbf{r})$  is the diameter of hard spheres located at position  $\mathbf{r}$ , and  $F_{HS}$  is the Helmholtz free energy of the hard-sphere fluid. The approximation for  $g_\sigma(\mathbf{r})$  is obtained by using the White Bear functional [20] for the Helmholtz free energy  $F_{HS}$  in Eq. 10. This provides an excellent approximation for this averaged value of the pair distribution function at contact for a variety of interfaces, and over a wide range of densities.

### IV. CONTACT VALUE APPROXIMATION

In the approaches for the pair distribution function mentioned above, the radial distribution function used in the approximation was dependent upon the density averaged over some volume. We seek to achieve greater accuracy by using instead a function dependent upon our averaged  $g_\sigma(\mathbf{r})$  discussed above, which holds more information about an inhomogeneous system than does a simple convolution of the density. We construct the CVA with the average of two radial distribution functions, evaluated at the distance between the two points, that are themselves functions of the averaged pair distribution function at contact  $g_\sigma(\mathbf{r})$  evaluated at the two points:

$$g^{(2)}(\mathbf{r}_1, \mathbf{r}_2) = \frac{g(r_{12}, g_\sigma(\mathbf{r}_1)) + g(r_{12}, g_\sigma(\mathbf{r}_2))}{2}. \quad (11)$$

This contact value approximation for  $g^{(2)}(\mathbf{r}_1, \mathbf{r}_2)$  is constructed to reproduce the exact value for the integral:

$$F_1^{\text{contact}} = \frac{1}{2} \iint g_{HS}^{(2)}(\mathbf{r}_1, \mathbf{r}_2) n(\mathbf{r}_1) n(\mathbf{r}_2) \delta(|\mathbf{r}_1 - \mathbf{r}_2| - \sigma) d\mathbf{r}_1 d\mathbf{r}_2 \quad (12)$$

which is the mean-field correction to the free energy (see Eq. 2) for a purely contact interaction.

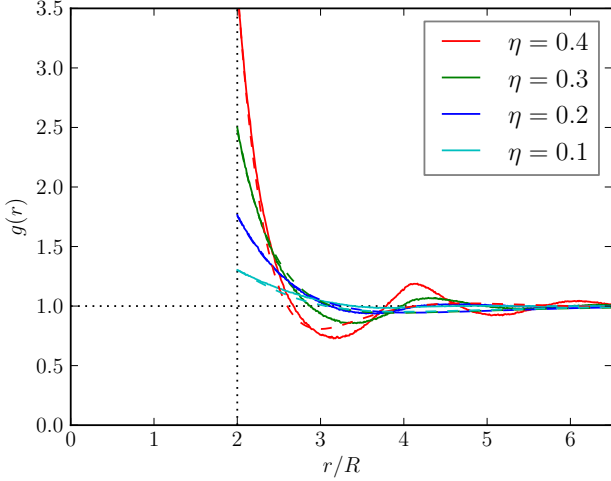


FIG. 1: Plot of the hard-sphere radial distribution function, with our separable fit. The solid lines show the true radial distribution function  $g(r)$ , and the dashed lines show our separable fit to the radial distribution functions  $g_S(r)$ .

The CVA requires the radial distribution function as a function of  $r$  and  $g_\sigma$ . One approach to constructing  $g(r, g_\sigma)$  is to compute  $\eta$  from  $g_\sigma$  and then find  $g(r, \eta)$  using either some approximate functional form (e.g. Percus-Yevick) or Monte Carlo simulation results. In this paper we first use the Monte Carlo results for the radial distribution function  $g(r)$ , which we also use in evaluating the approximations of earlier works.

## V. SEPARABLE RADIAL DISTRIBUTION FUNCTION FOR THE CVA-S

The CVA is quite accurate, but cannot be computed efficiently with fixed-kernel convolutions as written. In order to ease computational application of this pair distribution function in classical density functionals, we have developed a separable approximation for the function  $g(r, g_\sigma)$ :

$$g_S(|r_{12}|, g_\sigma) = \sum_i a_i(r_{12}) b_i(g_\sigma) \quad (13)$$

This separable contact value approximation (CVA-S) allows the mean field contribution to the free energy (Eq. 2) to be computed with only fixed-kernel convolutions, which can be efficiently computed using fast Fourier transforms.

We construct  $g_S(r, g_\sigma)$  to satisfy several constraints. Naturally, we match the value at contact:

$$g_S(\sigma, g_\sigma) = g_\sigma. \quad (14)$$

A second constraint applies to the integral of the total

correlation function,  $h(r) = g(r) - 1$ :

$$1 + n \int h(r) d\mathbf{r} = nkT\chi_T \quad (15)$$

where  $\chi_T$  is the isothermal compressibility of the hard-sphere fluid. We have found that the slope of the radial distribution function at contact is given to a very good approximation by:

$$g'(\sigma) \approx g_\sigma(1 - g_\sigma) \quad (16)$$

and we apply this as a final constraint.

Under these three constraints, we applied a least-squares fit to simulation data for the radial distribution function at packing fractions from 0.05 to 0.4 in steps of 0.05. Our fitted radial distribution function is given by

$$g_S(r, g_\sigma) = 1 + (g_\sigma - 1)e^{-\kappa_0(\frac{r}{\sigma} - 1)} + (g_\sigma - 1)(\kappa_0 - 2g_\sigma) \left(\frac{r}{\sigma} - 1\right) e^{-\kappa_1(\frac{r}{\sigma} - 1)} + I(g_\sigma) \left(\frac{r}{\sigma} - 1\right)^2 e^{-\kappa_2(\frac{r}{\sigma} - 1)} \quad (17)$$

$$I(g_\sigma) = \frac{\kappa_2^5 \frac{\chi-1}{24\eta} + (1-g_\sigma) \frac{(\kappa_0-2g_\sigma)(\kappa_1^2+4\kappa_1+6)}{\kappa_1^4} + (1-g_\sigma) \frac{\kappa_0^2+2\kappa_0+2}{\kappa_0}}{2\kappa_2^2 + 12\kappa_2 + 24} \quad (18)$$

$$\chi = \frac{(1-\eta)^4}{\eta^4 - 4\eta^3 + 4\eta^2 + 4\eta + 1} \quad (19)$$

Finally, we can convert between the packing fraction  $\eta$  and the radial distribution function at contact  $g_\sigma$  using the Carnahan-Starling approximation for  $g_\sigma$ :

$$g_\sigma = \frac{1 - \frac{\eta}{2}}{(1 - \eta)^3}, \text{ and its inverse} \quad (20)$$

$$\eta = 1 - \frac{1}{\sqrt[3]{54g_\sigma^2 - 6\sqrt{81g_\sigma^4 - 6g_\sigma^3}}} - \frac{\sqrt[3]{54g_\sigma^2 - 6\sqrt{81g_\sigma^4 - 6g_\sigma^3}}}{6g_\sigma}. \quad (21)$$

This function includes three fitted parameters,  $\kappa_0 = 3.68$ ,  $\kappa_1 = 2.16$ , and  $\kappa_2 = 2.79$ . The fit is displayed in Fig. 1. In that figure, it is apparent that the constraint on the integral of  $h(r)$  from Eq. 15 results in canceling errors at large distances. The maximum error in  $g_S(r)$  at packing fractions up to 0.4 is 0.19, which occurs at  $\eta = 0.4$  and  $r = 4.1R$ .

## VI. RESULTS

### A. Pair distribution function

We begin by examining the pair distribution function near a hard wall, with a focus on the case where one of the

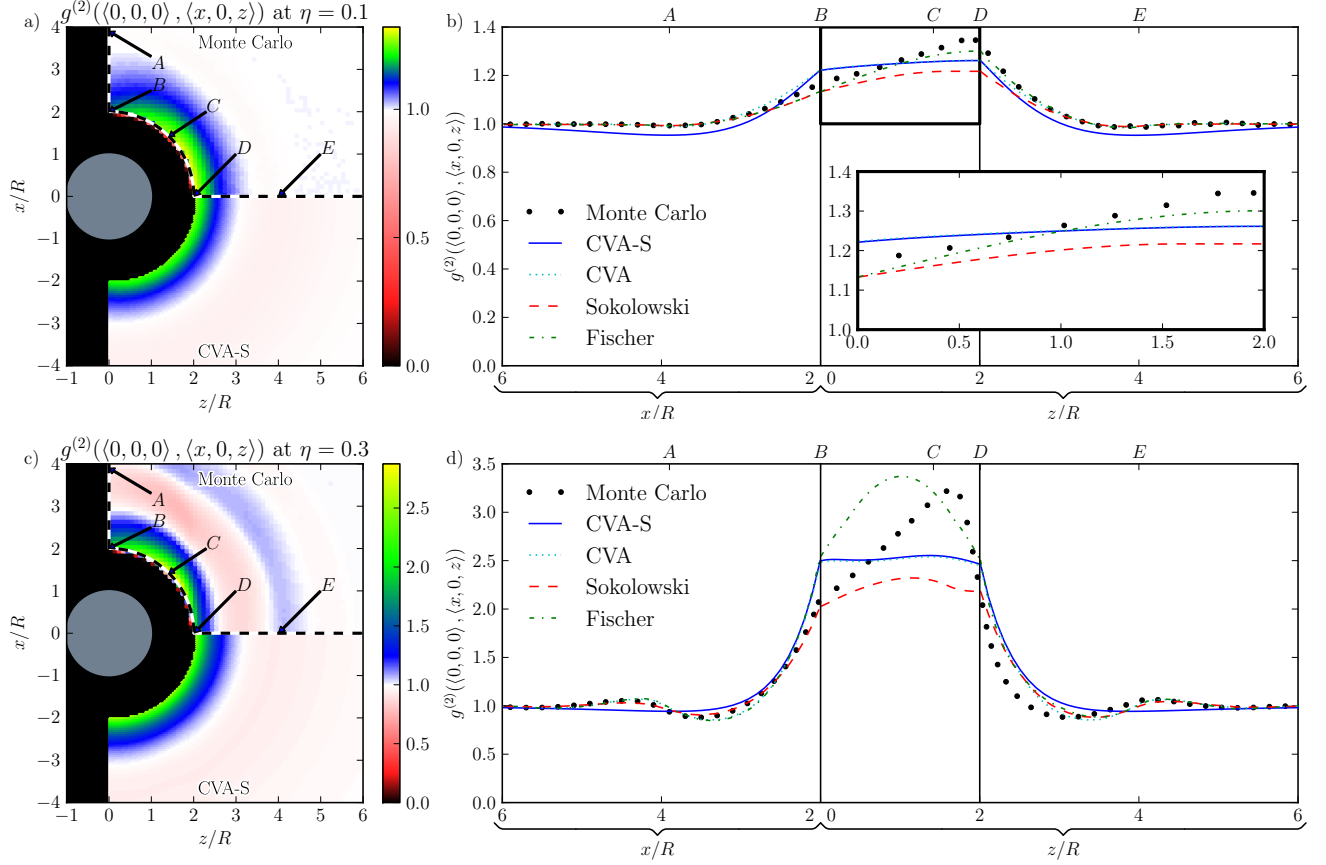


FIG. 2: The pair distribution function near a hard wall, with packing fractions of 0.1 and 0.3 and  $\mathbf{r}_1$  in contact with the hard wall. On the left are 2D plots of  $g^{(2)}(\mathbf{r}_1, \mathbf{r}_2)$  as  $\mathbf{r}_2$  varies. The top halves of these figures show the results of Monte Carlo simulations, while the bottom halves show the CVA-S. On the right are plots of  $g^{(2)}(\mathbf{r}_1, \mathbf{r}_2)$  on the paths illustrated in the figures to the left. These plots compare the CVA-S (blue solid line) and CVA (cyan dotted line) with Monte Carlo results (black circle) and the results of Sokolowski and Fischer (red dashed line) [18], and those of Fischer and Methfessel (green dot-dashed line) [16]. The latter is only plotted at contact, where it is defined.

two spheres is in contact with the hard wall. Figures 2a and 2c compare the results of the CVA-S with Monte Carlo simulations at packing fractions of 0.1 and 0.3 respectively. We see reasonable agreement at the lower density, with some reduced oscillations at larger distances, and a flatter angular dependence when the two spheres are in contact. At the higher density, we see significant structure developing in the simulation results that is not reflected in our approximation.

Figures 2b and 2d show the pair distribution function as plotted along paths illustrated in Figures 2a and 2c. These plots compare the CVA and CVA-S with Monte Carlo results, as well as the approximations of Sokolowski and Fischer [18] and of Fischer and Methfessel [16] at the same packing fractions of 0.1 and 0.3. The approach of Fischer and Methfessel is only defined when the two spheres are in contact, and is therefore only plotted on that segment of the path. As an input to both previous approximations and to the CVA, we use the hard sphere radial distribution function found with Monte Carlo simulation, interpolated as necessary. We find that both

previous approximations to the pair distribution function predict the qualitative angular dependence of the pair distribution function at contact better than this work. However, in each case the pair distribution function has a systematic error at contact—either too high or too low. While our approximation is smoother than either of the existing approaches, its errors will have a tendency to cancel when used in a perturbation expansion. At higher densities, the approximation of Fischer and Methfessel requires evaluating the radial distribution function at densities significantly higher than the freezing density, which poses numerical difficulties when using the radial distribution function from simulation. When the two points  $\mathbf{r}_1$  and  $\mathbf{r}_2$  are both more than a radius away from contact, we find that any of these approaches gives a reasonable prediction, with the CVA-S underestimating the oscillations in  $g^{(2)}$ , as expected based on the fit in Fig. 1.

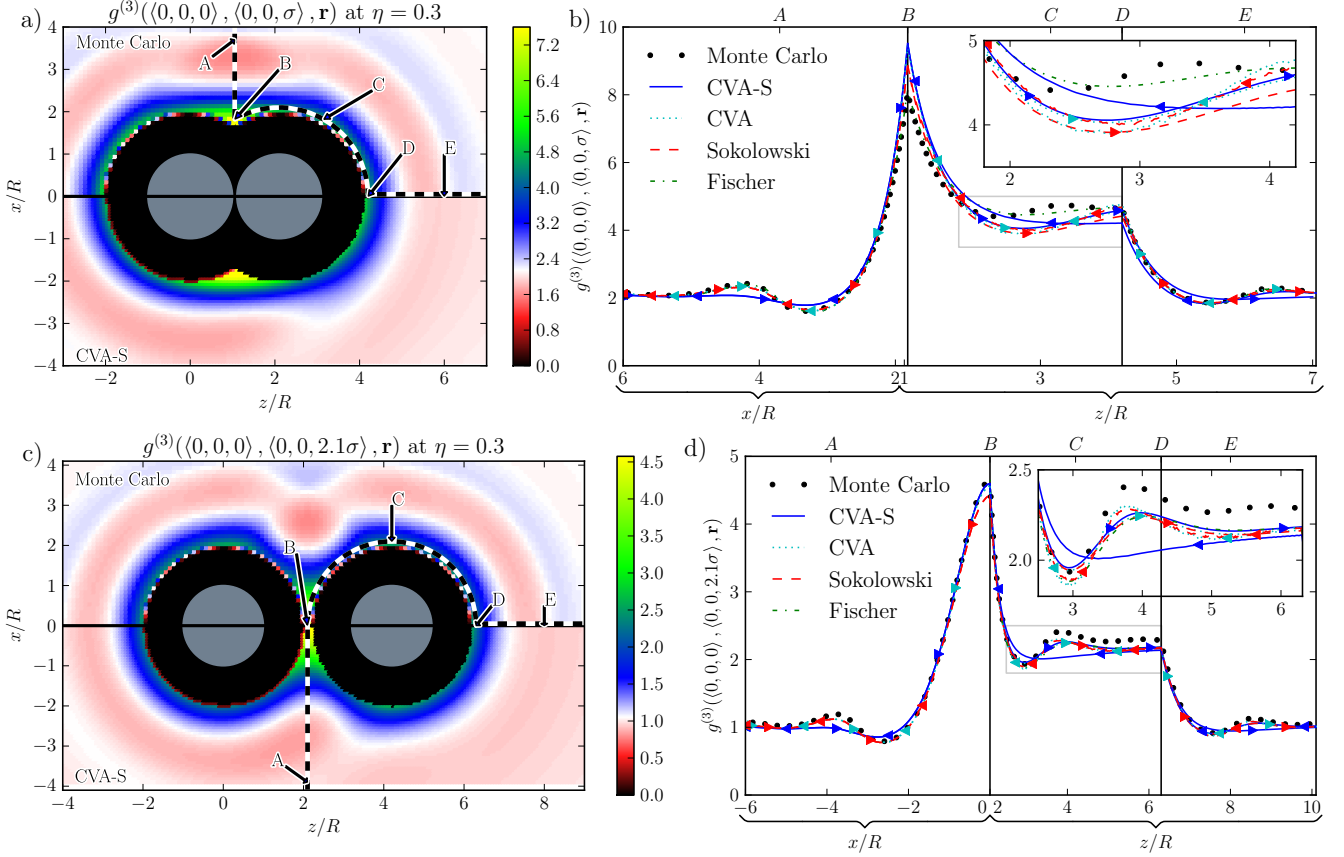


FIG. 3: The triplet distribution function  $g^{(3)}(\mathbf{r}_1, \mathbf{r}_2, \mathbf{r}_3)$  at packing fraction 0.3, plotted when  $\mathbf{r}_1$  and  $\mathbf{r}_2$  are in contact (a,b) and when  $\mathbf{r}_1$  and  $\mathbf{r}_2$  are separated by a distance  $2.1\sigma$  (c,d). On the left are 2D plots of  $g^{(3)}(\mathbf{r}_1, \mathbf{r}_2, \mathbf{r}_3)$  as  $\mathbf{r}_3$  varies. The top halves of these figures show the results of Monte Carlo simulations, while the bottom halves show the CVA-S. On the right are plots of  $g^{(3)}(\mathbf{r}_1, \mathbf{r}_2, \mathbf{r}_3)$  on the paths illustrated in the figures to the left. We also plot these curves along a left-right mirror image of this path. The data for the right-hand paths (as shown in the 2D images) are marked with right-pointing triangles, while the left-hand paths are marked with left-pointing triangles.

### B. Triplet distribution function

Just as the radial distribution function of a homogeneous fluid may be computed from the density of an inhomogeneous one using Percus' test-particle trick, the triplet distribution function of a homogeneous system can be computed using an approximation of the pair distribution for an inhomogeneous fluid, such as we have developed. The triplet distribution function of a homogeneous fluid with density  $n$  is given by:

$$g^{(3)}(\mathbf{r}_1, \mathbf{r}_2, \mathbf{r}_3) = \frac{n_{\text{TP}(\mathbf{r}_1)}(\mathbf{r}_2)n_{\text{TP}(\mathbf{r}_1)}(\mathbf{r}_3)}{n^2} g_{\text{TP}(\mathbf{r}_1)}^{(2)}(\mathbf{r}_2, \mathbf{r}_3) \quad (22)$$

where the  $\text{TP}(\mathbf{r}_1)$  subscript indicates quantities computed for the inhomogeneous density configuration in which one sphere (the “test particle”) is fixed at position  $\mathbf{r}_1$ . This method treats one of the three positions—the location of the test particle—differently from the other two, which means that a poor approximation to the pair

distribution function may break the symmetry between  $\mathbf{r}_1$  and  $\mathbf{r}_2$  which is present in the true triplet distribution function.

Figures 3a and 3c compare the triplet distribution function at a packing fraction of 0.3 computed using the CVA-S with results from Monte Carlo simulations. In Figure 3a the spheres at  $\mathbf{r}_1$  and  $\mathbf{r}_2$  are in contact; in Figure 3c they are spaced so that a third sphere can just fit between them; and in both figures  $\mathbf{r}_3$  is varied. The test-particle position for the CVA-S in each case is  $\mathbf{r}_1$ , which is on the left-hand side of the figure. We see reasonable agreement, with fewer oscillations in the CVA-S at larger distances. Also, the Monte Carlo results have the expected left-right symmetry, while the CVA-S has an asymmetry introduced with the test particle due to errors in the pair distribution function. Most notably, the CVA-S has less angular dependence at contact with the test particle than it does with the sphere at  $\mathbf{r}_2$ .

Figures 3b and 3d show the triplet distribution function as plotted along the paths illustrated in Figures 3a and 3c. We also plot the results along a left-right mir-

ror image path, corresponding to swapping  $\mathbf{r}_1$  and  $\mathbf{r}_2$ . The two mirror-image paths are distinguished by arrows (triangles) along the curves, with right-facing arrows indicating the paths shown in Figures 3a and 3c, and left-facing arrows indicating the mirror image path. As the work of Fischer and Methfessel is only defined when  $\mathbf{r}_2$  and  $\mathbf{r}_3$  are in contact, we only plot it along the central portion of the path, which is in contact with  $\mathbf{r}_2$ , and arrows are omitted. All methods perform similarly over this range with one exception. The separable CVA-S method once again underestimates the oscillations on the left-hand side of the curve, where  $\mathbf{r}_2$  and  $\mathbf{r}_3$  are separated by a large distance. On the path where  $\mathbf{r}_2$  and  $\mathbf{r}_3$  are closer, the CVA-S method compares favorably with the other approximations. This is consistent with Fig. 1, which shows that  $g_S(r)$  fits well the first peak of  $g(r)$ , but has fewer oscillations at large distances.

## VII. PERFORMANCE IN THERMODYNAMIC PERTURBATION THEORY

A particularly relevant quantitative test of a pair distribution function is how well it predicts the interaction energy due to a pair potential. To this end, we have computed the error in the first term in a high-temperature perturbation expansion  $F_1$  for several pair potentials. In order to focus on effects at the interface, we have defined a position-dependent pair interaction energy as

$$\frac{dF_1}{dz} = \frac{1}{2} \int g_{HS}^{(2)}(\mathbf{r}, \mathbf{r}') n(\mathbf{r}) n(\mathbf{r}') \Phi(|\mathbf{r} - \mathbf{r}'|) d\mathbf{r}' \quad (23)$$

which gives the contribution to the mean-field free energy due to molecules located in a plane of fixed  $z$ .

We plot this quantity for three representative pair potentials near a hard wall in Fig. 4. We have chosen to illustrate a delta-function interaction at contact (i.e. “sticky hard spheres”); a hard-core square-well fluid, with the length-scale of interaction taken from the optimal SAFT model for water found by Clark *et al.* [8]; and a  $1/r^6$  power-law attraction. These pair potentials represent a short-range interaction, a medium-range discontinuous interaction, and a long-range smooth interaction.

Figure 4a shows the results for the sticky hard-sphere fluid. The CVA and CVA-S are constructed to produce this result exactly, provided the averaged pair distribution function at contact from Ref. 19 is exact. As expected, we see excellent agreement with the Monte Carlo simulation results, while the approximations of Fischer and Sokolowski each show deviations near the interface. Figure 4b shows the same curve from Eq. 23 for the square-well fluid. This potential stresses the CVA-S, since the edge of the attraction occurs at the dip in the radial distribution function at this density, with poor results for the bulk fluid. We see that over these length scales, both the CVA and Sokolowski’s approximation are very accurate. Finally, in the case of the power-law attraction all approximations tested work very well.

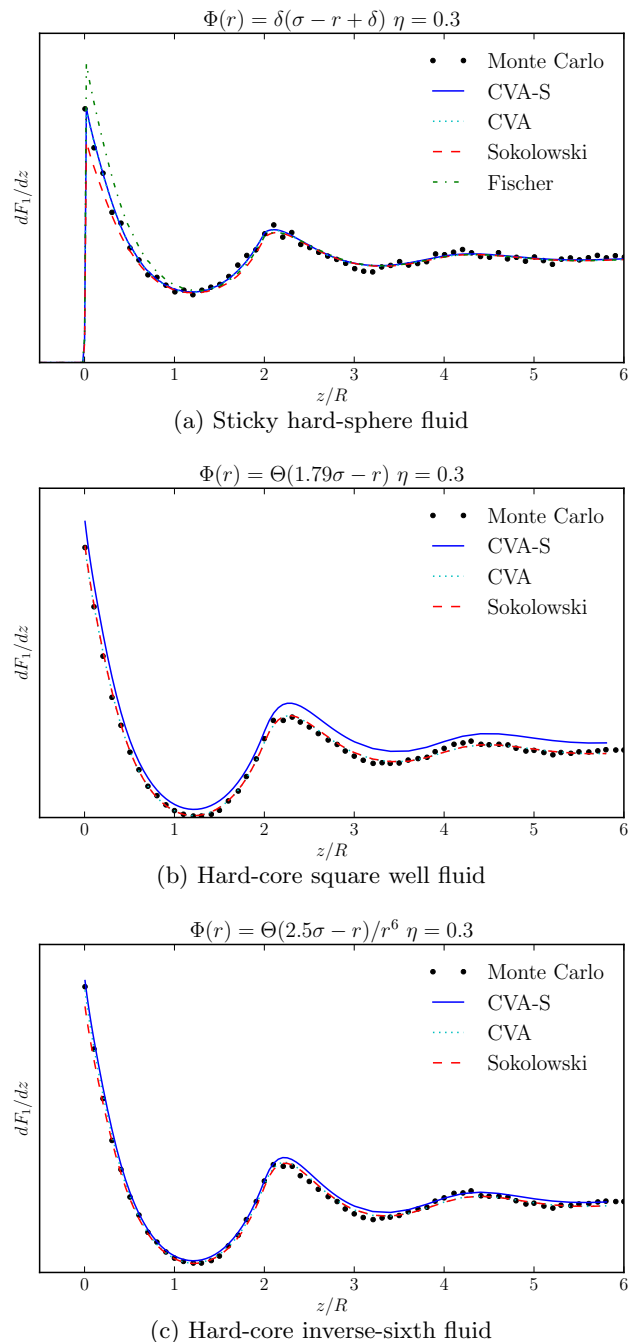


FIG. 4: Plot of  $\frac{dF_1}{dz}$  near a hard wall. (a) shows a sticky hard-sphere fluid defined by a pair potential  $\delta(\sigma - r + \delta)$  where  $\sigma$  is the hard-sphere diameter, and  $\delta$  is an infinitesimal distance; (b) shows a square well fluid defined by a pair potential  $\Theta(1.79\sigma - r)$ ; and (c) shows a hard-core inverse-sixth potential fluid with an attractive pair potential proportional to  $r^{-6}$ .

### VIII. CONCLUSION

We have introduced and tested the contact value approximation for the pair distribution function of the inhomogeneous hard-sphere fluid. The separable version of the contact value approximation is suitable for use in the development of classical density functionals constructed

using perturbation theory, as it may be efficiently computed using exclusively fixed-kernel convolutions. We have tested this function at a hard wall and near a single fixed hard sphere, and find that it gives qualitatively reasonable results. Tests of the pair distribution function in integrals that arise in thermodynamic perturbation theory suggest that our approximation is accurate for both short-range and long-range attractions.

- 
- [1] J. Hansen and I. McDonald, *Theory of Simple Liquids* (Elsevier Science, 2006).
  - [2] S. Jain, A. Dominik, and W. G. Chapman, *The Journal of chemical physics* **127**, 244904 (2007).
  - [3] G. J. Gloor, G. Jackson, F. Blas, E. M. Del Rio, and E. De Miguel, *The Journal of Physical Chemistry C* **111**, 15513 (2007).
  - [4] J. Gross, *The Journal of chemical physics* **131**, 204705 (2009).
  - [5] H. Kahl and J. Winkelmann, *Fluid Phase Equilibria* **270**, 50 (2008).
  - [6] J. Hughes, E. J. Krebs, and D. Roundy, *The Journal of Chemical Physics* **138**, 024509 (2013).
  - [7] P. Bryk, S. Sokolowski, and O. Pizio, *The Journal of chemical physics* **125**, 024909 (2006).
  - [8] G. Clark, A. Haslam, A. Galindo, and G. Jackson, *Molecular physics* **104**, 3561 (2006).
  - [9] R. Sundararaman, K. Letchworth-Weaver, and T. Arias, *The Journal of Chemical Physics* **137**, 044107 (2012).
  - [10] B. D. Marshall and W. G. Chapman, *The Journal of chemical physics* **138**, 044901 (2013).
  - [11] M. Plischke and D. Henderson, *Proceedings of the Royal Society of London. A. Mathematical and Physical Sciences* **404**, 323 (1986).
  - [12] B. Götzelmann, A. Haase, and S. Dietrich, *Physical Review E* **53**, 3456 (1996).
  - [13] R. Paul and S. Paddison, *Physical Review E* **67**, 016108 (2003).
  - [14] A. González, F. Román, and J. White, *Journal of Physics: Condensed Matter* **11**, 3789 (1999).
  - [15] F. Lado, *Molecular Physics* **107**, 301 (2009).
  - [16] J. Fischer and M. Methfessel, *Physical Review A* **22**, 2836 (1980).
  - [17] Y. Rosenfeld, *Physical review letters* **63**, 980 (1989).
  - [18] S. Sokolowski and J. Fischer, *The Journal of chemical physics* **96**, 5441 (1992).
  - [19] J. B. Schulte, P. A. Kreitzberg, C. V. Haglund, and D. Roundy, *Physical Review E* **86**, 061201 (2012).
  - [20] R. Roth, R. Evans, A. Lang, and G. Kahl, *Journal of Physics: Condensed Matter* **14**, 12063 (2002).